

Heterogeneous Catalysis in Solution

Part 23.¹—Kinetics of a Redox System

Showing Complete Mass-transport Control: The Hexacyanoferrate(III) + Iodide Reaction at a Rotating-platinum-disc Catalyst

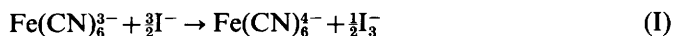
BY PAUL L. FREUND AND MICHAEL SPIRO*

Department of Chemistry, Imperial College of Science and Technology,
South Kensington, London SW7 2AY

Received 30th April, 1982

The rate of the reaction between Fe(CN)_6^{3-} and I^- has been measured from 5 to 30 °C in 1 mol dm⁻³ aqueous KNO_3 solution both homogeneously and in the presence of a large anodically preconditioned platinum-disc catalyst rotating from 100 to 2000 rev. min⁻¹. The catalytic rate agreed quantitatively with the mixture current (converted to a rate) at the point where the current-voltage curves of the two separate couples intersected; the mixture potential at this point also agreed well with the potential adopted by the catalysing disc. This confirmed the electrochemical mechanism of the platinum catalysis. That the catalytic process had become wholly mass-transport controlled was shown by the fact that the catalytic rates always varied proportionately with the square root of the angular velocity (ω) of the disc, while the catalyst potential remained independent of ω . Other predictions of the theory in the preceding paper to be fulfilled within experimental error were the kinetic orders of the heterogeneous reaction, the marked changes in these orders on adding the product Fe(CN)_6^{4-} to the initial mixture, and the negative Arrhenius activation energy associated with the catalytic rate constant.

Platinum metal strongly catalyses the redox reaction



as Just discovered in 1908.² A remarkable aspect of his discovery is that it was reached through theoretical insight: he was aware that the two couples involved were (in modern parlance) electrochemically reversible at a platinum electrode and he thereupon reasoned that the metal should catalyse the reaction between the couples. However, he believed – incorrectly – that the phenomenon originated in the oxidation and reduction of the platinum.

The catalysis of reaction (I) by platinum and other inert electron-conductors was subsequently confirmed by several other workers³⁻⁹ and as a result of their investigations the following facts are now known. (1) The rate of catalysis increases with faster stirring.^{6,8} (2) The variation with concentration of the mixture potential, E_{cat} , taken up by the platinum in the reaction mixtures could be quantitatively accounted for if reaction (I) reaches equilibrium rapidly at the catalyst surface but not in the bulk of the solution.⁵ (3) The value of E_{cat} observed in the reaction mixture was close to the potential at which the experimental current-voltage curves of the two separate couples (drawn with all currents as positive) intersected.⁸ Moreover, the mixture current density i_{mix} at the intersection agreed well with the catalytic rate, v_{cat} , with Faraday's constant F being used as the conversion factor.⁸ These experiments, incidentally, were carried out with an anodically pretreated platinum surface.

It would be difficult to explain the last set of experiments unless the redox reaction proceeded by an electrochemical mechanism whereby electrons are transferred from

I^- to $\text{Fe}(\text{CN})_6^{3-}$ through the platinum metal. Results (1) and (2) strongly suggest that reaction (I) is so fast at the platinum surface that the overall reaction becomes at least partly diffusion controlled. However, no-one has studied the kinetics of the catalysed reaction or investigated the effect of stirring speed quantitatively. It was our aim to remedy this deficiency and to see whether the results fitted the various theoretical predictions made in the preceding paper.¹ As a tool in this research we employed a large rotating-platinum-disc catalyst (r.d.c.) because the thickness of the diffusion layer at its surface is precisely known as a function of rotation speed.¹⁰

EXPERIMENTAL

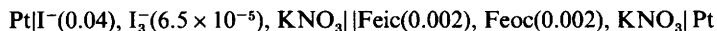
ELECTROCHEMICAL EXPERIMENTS

The large shiny circular platinum disc (geometrical area 11.2 cm^2) was made by brazing platinum foil onto a brass former of the trumpet shape recommended on hydrodynamic grounds.¹¹ The brass was insulated from the solution by covering it with white enamel paint (International Radiator) that was baked on for 2 h at 100°C . The disc was always electrochemically preconditioned in deoxygenated $1 \text{ mol dm}^{-3} \text{ H}_2\text{SO}_4$ at the temperature of the subsequent electrochemical or kinetic experiments, using the sequence $+1.56 \text{ V}$ for 10 s, $+0.96 \text{ V}$ for 40 s, -0.16 V for 3 s and $+1.40 \text{ V}$ for 10 min, based on the potential programme 1A of Gilroy.¹² During the first two steps the disc was rotated at $500 \text{ rev. min}^{-1}$. Speeds were set with a Servomex motor controller MC 43 and were checked with a stroboscopic disc or with a Racal universal counter 835 attached to a Racal tachometer MA 38. Potentials were measured relative to a saturated calomel (SCE) reference electrode (E.I.L.) and so recorded.

Steady-state current-voltage curves for each couple were carried out with a Chemical Electronics TR70/2A potentiostat. Potentials were set manually, and the currents determined by measuring the drop in voltage (on a Hewlett Packard 3440 A digital voltmeter) across a calibrated 400Ω resistor (Croydon Precision Instruments type RBB1) connected in series with the cell. The disc compartment of the electrolysis cell held *ca.* 250 cm^3 solution with a large platinum-foil counter-electrode placed flat on the bottom. The reference electrode ended in a vertical Luggin capillary underneath the disc centre and filled with the cell solution. Nitrogen was bubbled through the solution before each experiment, and the ferricyanide (or iodide) solution then electrolysed at constant current to generate the small amounts of ferrocyanide ($2 \mu\text{mol dm}^{-3}$) or iodine ($1 \mu\text{mol dm}^{-3}$) required for the respective current-voltage curves.

The limiting current densities L_i for the 4 reactants and products were measured as a function of their concentrations c ($\leq 0.003 \text{ mol dm}^{-3}$) in separate runs at $500 \text{ rev. min}^{-1}$ in $1 \text{ mol dm}^{-3} \text{ KNO}_3$ at 5°C , in order to determine their mass-transport rate constants k_j .

The difference between the formal potentials of the two couples, $E_2^\circ - E_1^\circ$, was obtained at various KNO_3 concentrations over the temperature range $5\text{--}30^\circ\text{C}$ from the e.m.f. of the cell



where the bracketed numbers represent the concentrations in mol dm^{-3} . Here $[\text{I}_3^-] = [\text{I}^-]^3$, and Feic and Feoc are abbreviations for $\text{K}_3\text{Fe}(\text{CN})_6$ and $\text{K}_4\text{Fe}(\text{CN})_6$, respectively. The e.m.f. values of the two half-cells were also measured against the same SCE to provide separate values of E_1° and E_2° .

KINETIC RUNS

All the chemicals used were of AnalaR grade. The flanged Pyrex reaction vessel (Quickfit FV 500), i.d. 7.5 cm , was well immersed in an insulated water thermostat bath cooled at temperatures below ambient by a Townson and Mercer refrigeration unit. Most experiments were carried out at $5 \pm 0.02^\circ\text{C}$, where the correction for the homogeneous reaction was small. In a typical catalytic run, 200 cm^3 of thermostatted KI solution were pipetted into the reaction vessel and the rotating disc lowered to 2 cm below the surface. (Prior nitrogen bubbling was found to have no effect on the rate.) The SCE was inserted, and the digital voltmeter connected between it and the disc to record the latter's potential during the run. The disc was set in motion

at the required speed; in homogeneous runs the solutions were stirred with an immersible magnetic stirrer. After thermal equilibration the reaction was initiated by adding 10 cm³ potassium ferricyanide solution. All solutions contained KNO₃ at the appropriate concentration (usually 1 mol dm⁻³ but less at higher KI molarities so as to keep the ionic strength at 1.05 mol dm⁻³). If one of the products was to be present at the start, the desired amount of iodine or ferrocyanide was generated by first placing an iodide or ferricyanide solution, respectively, in the reaction vessel and passing the requisite number of coulombs through an auxiliary platinum electrode, the counter-electrode being in an adjoining vessel connected with a salt bridge.

Both homogeneous and catalysed reactions were followed by removing 5 cm³ aliquots at suitable time intervals. Each aliquot was diluted with 10 cm³ supporting electrolyte solution at the experimental temperature, so effectively stopping the reaction, and poured into a 4 cm quartz cuvette. The reference cuvette held a blank solution containing the same concentration of ferricyanide (one-third that in the reaction mixture). The absorbance of I₃⁻ in the sample was then determined at 350 nm in a Unicam SP 1800 spectrophotometer. The effective extinction coefficient was taken as

$$\epsilon_{\text{eff}} = \frac{\epsilon(\text{I}_3^-)[\text{I}_3^-]}{[\text{I}_3^-] + [\text{I}_2]} = \frac{\epsilon(\text{I}_3^-)}{1 + 1/K_s[\text{I}^-]_{\text{eff}}} \quad (1)$$

where the square brackets denote concentration, $[\text{I}^-]_{\text{eff}}$ the diluted iodide concentration in the sample cell, K_s is the stability constant of I₃⁻ (taken from data¹³ in 1 mol dm⁻³ HClO₄ extrapolated to lower temperatures by an Arrhenius plot), and $\epsilon(\text{I}_3^-)$ its extinction coefficient in 1 mol dm⁻³ KNO₃ at 350 nm. This was found to be $2.53 \times 10^4 \text{ dm}^3 \text{ mol}^{-1} \text{ cm}^{-1}$, in reasonable agreement with other values obtained in this laboratory^{6, 8} (2.50×10^4 , 2.63×10^4) and elsewhere¹⁴ (2.43×10^4 without added KNO₃). The optical contribution of the molecular iodine was negligible because of its much smaller extinction coefficient (*ca.* 600, *cf.* 170¹⁴) and its low concentration in the sample solutions. The difference $\epsilon(\text{Feic}) - \epsilon(\text{Feoc})$ (130,⁶ 134¹⁴) was also small enough to be neglected.

In most kinetic runs, 8 aliquots of 5 cm³ each were removed for analysis from an initial volume of 210 cm³. In the catalytic runs this withdrawal of samples meant that the iodine formed at the platinum surface was distributed in progressively smaller volumes of solution, so creating an artificially rising rate constant. This problem was overcome with an appropriate correction function. The homogeneous rate v_{hom} (in mol dm⁻³ s⁻¹) and the heterogeneous rate v_{cat} (in mol m⁻² s⁻¹) can be taken as constant in a given experiment, since only a small fraction of the reactants had been consumed when the last sample was taken (typically 3½% of the ferricyanide and 0.1% of the iodide). Suppose the initial tri-iodide ion concentration (or the effective background) is c_0 and that it rises to c_1 after a time interval Δt_1 . Then

$$c_1 = c_0 + v'_{\text{hom}} \Delta t_1 + \frac{v'_{\text{cat}} A \Delta t_1}{V_0} \quad (2)$$

where v'_{hom} and v'_{cat} here refer to the formation of moles of I₃⁻, and where A is the catalyst area and V_0 the initial volume of the reaction mixture. The first aliquot of size ΔV is then removed. After a further time interval Δt_2 the product concentration will have increased to c_2 , where

$$c_2 = c_1 + v'_{\text{hom}} \Delta t_2 + \frac{v'_{\text{cat}} A \Delta t_2}{V_0 - \Delta V} \quad (3)$$

In general

$$c_j = c_{j-1} + v'_{\text{hom}} \Delta t_j + \frac{v'_{\text{cat}} A \Delta t_j}{V_0 - (j-1) \Delta V} \quad (4)$$

On addition

$$c_j = c_0 + v'_{\text{hom}} \sum_1^j \Delta t_i + v'_{\text{cat}} A S_j \quad (5)$$

where

$$S_j = \sum_1^j \frac{\Delta t_i}{V_0 - (i-1) \Delta V}.$$

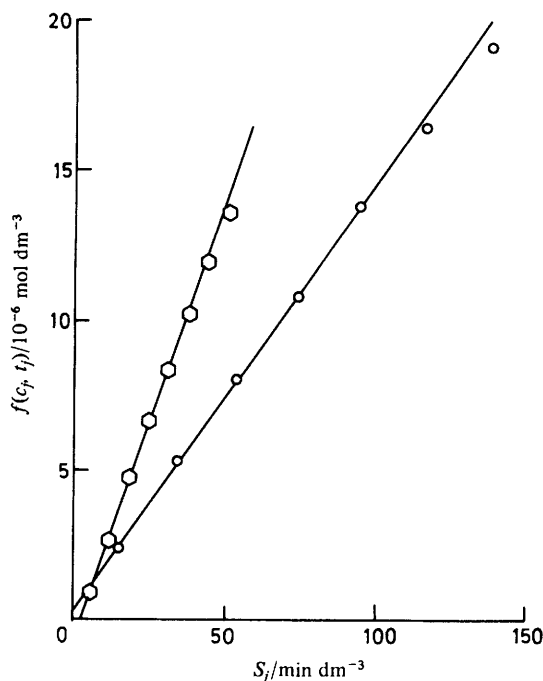


FIG. 1.—Kinetic plots of two catalysed runs with the standard solution of $1 \times 10^{-3} \text{ mol dm}^{-3}$ Feic, 0.05 mol dm^{-3} KI and 1 mol dm^{-3} KNO_3 at 5°C . The upper curve refers to the disc rotating at $2000 \text{ rev. min}^{-1}$ and the lower at $500 \text{ rev. min}^{-1}$.

Plots of $c_j - v'_{\text{hom}} \sum_1^j \Delta t_i$ [abbreviated to $f(c_j, t_j)$] against S_j were accordingly drawn for each catalytic run. These plots curved gently (*cf.* fig. 1) which indicated a slow decrease in $v'_{\text{cat}} A$, and the data were therefore fitted by least squares to a second-order polynomial of the form

$$f(c_j, t_j) = c_0 + v'_{\text{cat}} A S_j - a S_j^2 \quad (6)$$

to furnish values for v'_{cat} at zero time. These values were found to be independent of V_0 from 0.2 to 0.8 dm^3 with the platinum disc used. In the homogeneous runs the concentration against time plots were quite linear during the first 80–100 min of reaction.

RESULTS AND DISCUSSION

HOMOGENEOUS REACTION

The initial homogeneous velocities at 5°C in 1 mol dm^{-3} KNO_3 fitted the equation

$$v_{\text{hom}}/\text{mol dm}^{-3} \text{ s}^{-1} = 2d[\text{I}_3^-]/dt = 5.1_5 \times 10^{-4} [\text{Feic}] [\text{I}^-]^2 \quad (7)$$

over the range $(1.3) \times 10^{-3} \text{ mol dm}^{-3}$ $\text{K}_3\text{Fe}(\text{CN})_6$ and 0.05 – 0.1 mol dm^{-3} KI. A third-order dependence of this kind was first reported by Just² and has since been confirmed by several other authors.⁷ The rate was found to decrease on adding up to $1 \times 10^{-3} \text{ mol dm}^{-3}$ $\text{K}_4\text{Fe}(\text{CN})_6$ initially. To a good approximation its effect on a 'standard' reaction mixture of $1 \times 10^{-3} \text{ mol dm}^{-3}$ Feic + 0.05 mol dm^{-3} KI in 1 mol dm^{-3} KNO_3 at 5°C could be represented by dividing the right-hand side of eqn (7) by

$$(1 + 0.9[\text{Feoc}]/[\text{Feic}])$$

a form suggested by previous work in the literature.¹⁵ However, the rate was not affected by addition of up to 1×10^{-4} mol dm⁻³ iodine to the reaction mixture when allowance was made for the increasing difficulty in measuring accurately the absorbance changes with time under these circumstances.

In 0.5 and 1.5 mol dm⁻³ KNO₃ at 5 °C the third-order rate constants k_3 were, respectively, 2.9×10^{-4} and 6.8×10^{-4} dm⁶ mol⁻² s⁻¹. Majid and Howlett⁷ found that their third-order rate constants varied linearly with [K⁺] up to *ca.* 0.5 mol dm⁻³. We find this to be only approximately true at higher concentrations even when association between K⁺ and NO₃⁻ has been taken into account. Using a value of $K_{\text{ass}} = 1.1 \pm 0.1$ dm³ mol⁻¹, obtained by extrapolating two sets of literature values at zero ionic strength¹⁶ to 5 °C, and stoichiometric activity coefficients¹⁷ at 25 °C, we calculated k_4 to be $(6.3, 6.2 \text{ and } 5.7) \times 10^{-4}$ dm⁹ mol⁻³ s⁻¹ in 0.5, 1.0 and 1.5 mol dm⁻³ KNO₃, respectively. Majid and Howlett⁷ reported a value for k_4 of 7.1×10^{-4} dm⁹ mol⁻³ s⁻¹ at 5 °C at ionic strengths up to 0.5.

Initial rates of 'standard' reaction mixtures were determined at 5 °C intervals from 5 to 30 °C inclusive. The third-order rate constants could be satisfactorily fitted by the Arrhenius equation

$$k_3/\text{dm}^6 \text{ mol}^{-2} \text{ s}^{-1} = 8.80 \times 10^3 \exp(-4625/T). \quad (8)$$

The activation energy E^\ddagger of 38.4 kJ mol⁻¹ agrees moderately well with the values of Majid and Howlett⁷ of 35.1 and of Hussain and Howlett¹⁸ of 37 kJ mol⁻¹. At 25 °C our value of k_4 (corrected for ionic association¹⁶ with $K_{\text{ass}} = 0.65$ dm³ mol⁻¹) of 17.4×10^{-4} dm⁹ mol⁻³ s⁻¹ is again lower than the value of Majid and Howlett⁷ of 18.8×10^{-4} , while extrapolation of our data to 0 °C yields $v_{\text{hom}} = 0.98 \times 10^{-9}$ dm³ mol⁻¹ s⁻¹, in good agreement with the figure of Spiro and Griffin⁸ of 1.02×10^{-9} .

PROPERTIES OF REACTANTS AND PRODUCTS

Before the catalysed reaction can be discussed, the values of certain parameters of the general theory¹ must be specified for the system under study. Table 1 lists the stoichiometric coefficients ν_j of the reactants and products of reaction (I), as well as the mass-transport rate constants k_j determined from the limiting current densities L_j by eqn (6) of ref. (1).

The trace diffusion coefficients D_j in the last column were calculated from eqn (5) and (10) of ref. (1) by taking the viscosity of 1 mol dm⁻³ KNO₃ solution at 5 °C as¹⁹ $1.39_5 \times 10^{-3}$ kg m⁻¹ s⁻¹, its density as²⁰ 1063.7 kg m⁻³, and its kinematic viscosity as 1.312×10^{-6} m² s⁻¹. Trace diffusion data for these ions in the literature are available

TABLE 1.—CERTAIN PROPERTIES OF REACTANTS AND PRODUCTS IN 1 mol dm⁻³ KNO₃ AT 5 °C

species <i>j</i>		ν_j^a	k_j^b /10 ³ A dm ³ mol ⁻¹ m ⁻²	D_j /10 ⁻¹⁰ m ² s ⁻¹	$D_j\eta/T$ /10 ⁻¹⁵ kg m s ⁻¹ K ⁻¹
theory	expt.				
Ox ₂	Feic	1	2.38	4.36	2.19
Red ₁	I ⁻	$\frac{3}{2}$	4.21	10.26 ^c	5.15
Red ₂	Feoc	1	2.17	3.80	1.91
Ox ₁	I ₃ ⁻	$\frac{1}{2}$	5.88	5.99	3.00

$$^a \phi = 1/(\nu_{\text{Feoc}} + \nu_{\text{I}_3^-}) = \frac{2}{3}; \quad ^b \text{ at } 500 \text{ rev. min}^{-1}; \quad ^c \nu_j = 1.$$

only in other supporting electrolytes and at other temperatures (mainly 25 °C). To be able to make comparisons we must resort to the approximate Stokes–Einstein equation

$$D_j = kT/6\pi r_j \eta \quad (9)$$

where k is the Boltzmann constant, η the viscosity of the medium and r_j the effective radius of ion j . If r_j is assumed not to vary, then $D_j\eta/T$ should remain approximately constant for a given ion in a supporting electrolyte of the same ionic strength. Table 1 therefore lists our values of $D_j\eta/T$. The following values of $10^{15}D_j\eta/T$ are available in the literature, mainly from data at 25 °C and all in media that are 1 mol dm⁻³ in K⁺ ion:

Feic:	2.27 (KCl), ²¹	2.1 (KCl), ²²	2.00 (KCl), ²³	2.76 (KOH), ²⁴	2.35 (KOH), ²⁵
	2.40 (K ₂ SO ₄). ²²				
Feoc:	1.88 (KCl), ²¹	1.5 (KCl), ²²	1.74 (KCl), ²³	2.44 (KOH), ²⁴	1.90 (KOH), ²⁵
	1.63 (K ₂ SO ₄). ²²				
I ⁻ :	5.43 (KI), ²⁶	5.58 (KI), ²⁷	5.71 (KCl). ²⁸		
I ₃ ⁻ :	2.94 (KI). ¹¹				

Where viscosities were not given in the papers cited, they were taken from the compilation by Stokes and Mills.²⁹ It is quite apparent that there are wide variations in the literature even for the same supporting electrolyte at a given temperature. With the exception of I⁻, our own data in table 1 fit well inside the range of reported figures.

TABLE 2.—FORMAL POTENTIALS OF THE TWO COUPLES IN 1 mol dm⁻³ KNO₃ MEASURED AGAINST A SATURATED CALOMEL ELECTRODE

$T/^{\circ}\text{C}$	E_1°/V	E_2°/V	$(E_2^{\circ} - E_1^{\circ})/\text{V}^a$
5	0.3000	0.2598	-0.0404
10	0.3021	0.2514	-0.0508
15	0.3031	0.2425	-0.0606
20	0.3039	0.2333	-0.0706
25	0.3043	0.2244	-0.0800
30	0.3044	0.2156	-0.0889

^a Directly measured difference between the two half cells.

Table 2 gives the values of the equilibrium potentials of the two couples over a range of temperatures. In view of the high and constant KNO₃ concentration and the low concentrations of the electroactive species, the potentials may be taken to be the formal potentials of the couples concerned. The directly measured differences $E_2^{\circ} - E_1^{\circ}$ are seen to agree to 0.2 mV or better with the differences obtained by subtracting the separately measured values on paper.

KINETICS OF THE CATALYSED REACTION

Fig. 2 depicts the variation of v_{cat} with $f^{\frac{1}{2}}$, where $f (= \omega/2\pi)$ is the rotation speed of the disc in Hz, for the 'standard' reaction mixture. Such plots were always straight lines passing through the origin, a clear indication of total transport control. At the platinum surface, therefore, the reaction was very fast and had effectively come to equilibrium. This is borne out by the fact that the potential of the platinum disc, E_{cat} , became stable almost immediately after the start and then fell by only *ca.* 1 mV during

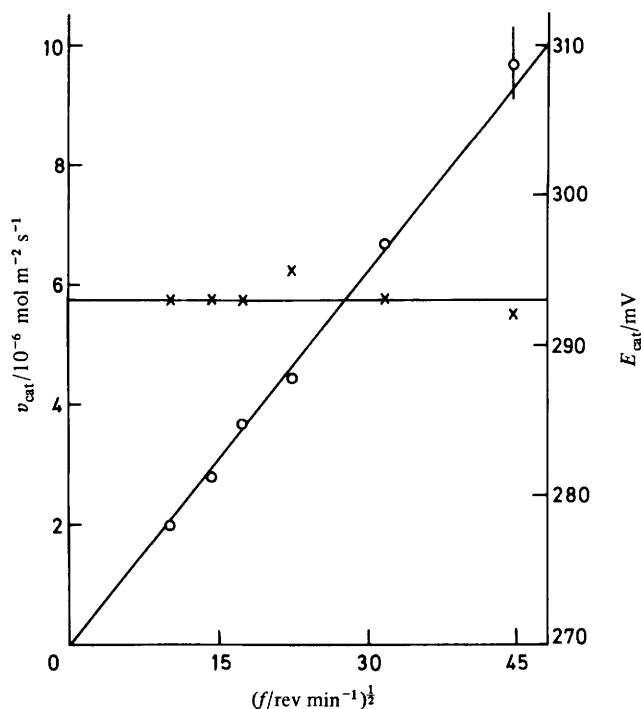


FIG. 2.—Variation of v_{cat} (O) and E_{cat} (x) with the square root of the rotation speed, for the standard reaction mixture at 5 °C.

TABLE 3.—EFFECT ON v_{cat} AND E_{cat} OF CHANGES IN THE REACTANT CONCENTRATIONS IN 1 mol dm⁻³ KNO₃ AT 5 °C AT A ROTATION SPEED OF 500 rev. min⁻¹

[Feic] /10 ⁻³ mol dm ⁻³	[I ⁻] /10 ⁻³ mol dm ⁻³	v_{cat} /10 ⁻⁶ mol m ⁻² s ⁻¹	$v_{\text{cat}}^{\text{calc}}$ /10 ⁻⁶ mol m ⁻² s ⁻¹	E_{cat} /mV	$E_{\text{cat}}^{\text{calc}}$ /mV
0.2	50	1.27	1.41	279	280
0.5	50	2.59	2.73	286	288
1.0	50	4.43	4.47	295	294
2.0	50	6.64	7.26	299	300
5.0	50	12.2	13.7	307	307
1.0	30	2.59	2.81	306	307
1.0	50	4.43	4.47	295	294
1.0	80	6.57	6.66	283	282
1.0	150	10.4	10.8	263	265
1.0	300	10.4	16.7	241	244

the 30 min of reaction. In fig. 2 E_{cat} is seen to be independent of rotation speed, as predicted by eqn (34) of the preceding paper.¹

The catalytic performance of the disc, as measured by v_{cat} , remained remarkably constant during the course of this work (> 2 years). Some white specks gradually accumulated on the surface but these could be wiped off with paper tissue. As stated earlier, the disc was electrochemically preconditioned before each run.

Table 3 sets out the effect on v_{cat} and on E_{cat} of changes in the reactant concentrations under our normal conditions of 1 mol dm⁻³ KNO₃ at 5 °C with the disc spinning at 500 rev. min⁻¹. The reaction orders can now be determined with the help of the appropriate theory. According to eqn (3), (6) and (33) of ref. (1)

$$\frac{1}{v_{\text{cat}}} = \frac{F}{W} + \frac{2F}{3k_{\text{Feic}}c_{\text{Feic}}} + \frac{F}{k_{\text{I}^-}c_{\text{I}^-}} \quad (10)$$

where F is Faraday's constant and W is given by

$$W = k_{\text{I}_3^-}^{\frac{1}{2}} k_{\text{Feoc}}^{\frac{1}{2}} c_0 \left(\frac{[\text{Feic}]}{c_0} \right)^{\frac{2}{3}} \left(\frac{[\text{I}^-]}{c_0} \right) \exp \frac{2F(E_2^\circ - E_1^\circ)}{3RT}. \quad (11)$$

The factor c_0 , equal to 1 mol dm⁻³, has been included for dimensional reasons. {Its origin lies in the theoretical equations (26) and (27) of ref. (1), in which all the concentrations are relative ones and should properly be written $[]/c_0$.} The last term on the right-hand side of eqn (10) is very small, and we have therefore plotted $\ln(1/v_{\text{cat}} - 2F/3k_{\text{Feic}}c_{\text{Feic}})$ against $\ln c_{\text{Feic}}$ at constant c_{I^-} , and *vice versa*. The slopes of the resulting straight lines yielded a reaction order for Feic of 0.66 ± 0.03 and for I⁻ of 1.02 ± 0.01 , in excellent agreement with the theoretical predictions of eqn (11). There is independent confirmation from the work of Hussain and Howlett.¹⁸ Using platinum foil mounted vertically on a variable-speed stirrer, they found at 10 °C with $[\text{K}^+] = 0.328$ mol dm⁻³ that the order of the catalysed reaction was *ca.* 0.7 with respect to ferricyanide and 1.0 with respect to iodide.

The expected rate constant of the W/F term in eqn (11) is 10.18×10^{-3} mol m⁻² s⁻¹, as calculated from the independently measured k_j values in table 1 and the formal potential data in table 2. It is now possible to test the electrochemical theory in absolute terms by predicting the catalytic rates from eqn (10). Table 3 shows that the agreement between the experimental and the calculated v_{cat} values is reasonably satisfactory. Although the theoretical values are always larger, the difference only exceeds the joint experimental uncertainties for the 0.3 mol dm⁻³ KI solution. Here the ionic medium has changed appreciably (to 0.3 mol dm⁻³ KI + 0.75 mol dm⁻³ KNO₃) and this is likely to have altered such theoretical parameters as $(E_2^\circ - E_1^\circ)$.

The potential adopted by the catalysing platinum disc provides a separate test of the theory. According to eqn (34) of ref. (1), E_{cat} should to a first approximation vary linearly with $\ln[\text{Feic}]$ with a slope of $RT/3F$ ($= 7.99$ mV at 5 °C) and also with $\ln[\text{I}^-]$ with a slope of $-RT/F$ (-24.0 mV). The same prediction was made earlier⁵ on a simple model of equilibrium at the platinum surface. The experimental E_{cat} values in table 3 do show a linear variation with $\ln[\text{Feic}]$ with a slope of 8.2₅ mV and with $\ln[\text{I}^-]$ (at the lower concentrations) with a slope of -23.2 mV. The agreement is therefore quite good. A better test is possible by using the complete eqn (34).¹ The values of i_{mix} in the last two terms were calculated from eqn (27) and (28) of ref. (1) using the independently measured values of k_j ($= L_j/c_j$) and E° (tables 1 and 2). The last two columns of table 3 now demonstrate that the experimental and predicted catalyst potentials agree well at all concentrations. The biggest difference, of 3 mV, is again shown by the 0.3 mol dm⁻³ KI solution.

Table 4 summarises the kinetic parameters given by the theory for various experimental conditions. Some of the most surprising predictions are the marked changes in reaction orders when one of the products is added to the initial reaction mixture. Several sets of experiments were therefore carried out to test these predictions. Table 5 lists the results when the product added was Feoc. The initial catalytic rate of the standard reaction mixture is seen to fall steadily the more ferrocyanide is

TABLE 4.—PREDICTED KINETIC PARAMETERS FOR THE CATALYSED REACTION (I) UNDER TOTAL MASS-TRANSPORT CONTROL

condition	reaction orders w.r.t.				catalytic rate constant ^a / $10^{-3} \text{ mol m}^{-2} \text{ s}^{-1}$
	Feic	I ⁻	Feoc	I ₃ ⁻	
no added product	$\frac{2}{3}$	1	0	0	10.18 ^b
added Feoc	2	3	-2	0	2.09
added I ₃ ⁻	1	$\frac{3}{2}$	0	$-\frac{1}{2}$	4.16

^a In $1 \text{ mol dm}^{-3} \text{ KNO}_3$ at 5°C at $500 \text{ rev. min}^{-1}$; ^b For the W/F term.

TABLE 5.—EFFECT ON v_{cat} AND E_{cat} OF THE ADDITION OF FERROCYANIDE IN $1 \text{ mol dm}^{-3} \text{ KNO}_3$ AT 5°C AND AT $500 \text{ rev. min}^{-1}$

[Feic] / $10^{-3} \text{ mol dm}^{-3}$	[I ⁻] / $10^{-3} \text{ mol dm}^{-3}$	[Feoc] / $10^{-3} \text{ mol dm}^{-3}$	v_{cat} / $10^{-6} \text{ mol m}^{-2} \text{ s}^{-1}$	E_{cat} /mV	$E_{\text{cat}}^{\text{calc}}$ /mV	E_2^{calc} /mV
1.0	50	0.001	4.27	294	294	425
1.0	50	0.01	4.13	293	294	370
1.0	50	0.1	3.05	290	290	315
1.0	50	0.2	2.07	286	286	286
1.0	50	0.4	0.99	278	278	278
1.0	50	0.6	0.47	271	270	270
1.0	50	1.0	0.08	259	259	260
0.5	50	0.4	0.22	263	264	265
0.7	50	0.4	0.44	270	271	273
1.0	50	0.4	0.99	278	278	282
1.5	50	0.4	1.79	285	285	292
2.0	50	0.4	2.84	290	290	298
1.0	30	0.4	0.19 ₅	280	281	282
1.0	32	0.4	0.26	279	280	282
1.0	34	0.4	0.48	280	280	282
1.0	37	0.4	0.57	279	280	282
1.0	40	0.4	0.60	280	279	282
1.0	50	0.4	0.99	278	278	282
1.0	60	0.4	1.56	277	276	282
1.0	70	0.4	2.09	274	274	282

present, and the corresponding log/log plot is drawn in fig. 3. Within the large experimental uncertainties associated with the very slow rates, the slope at the higher Feoc concentrations is clearly consistent with the theoretical prediction of -2 (table 4). Other log/log plots constructed for the variation of v_{cat} with [Feic] and with [I⁻] at a constant initial Feoc concentration of $4 \times 10^{-4} \text{ mol dm}^{-3}$ yield gentle curves with mean slopes of 1.7_5 and 2.8 , respectively. These orders of reaction are much higher than those found in the absence of added Feoc and approach the predicted values of 2 and 3, respectively, in table 4. It seems likely that even better agreement with the theoretical requirements would be obtained at higher Feoc concentrations. Table 5 also shows that the theory, in the form of eqn (26b), (27) and (28) of ref. (1), accounts quantitatively for the fall in the catalyst's potential as ferrocyanide is added. In fact,

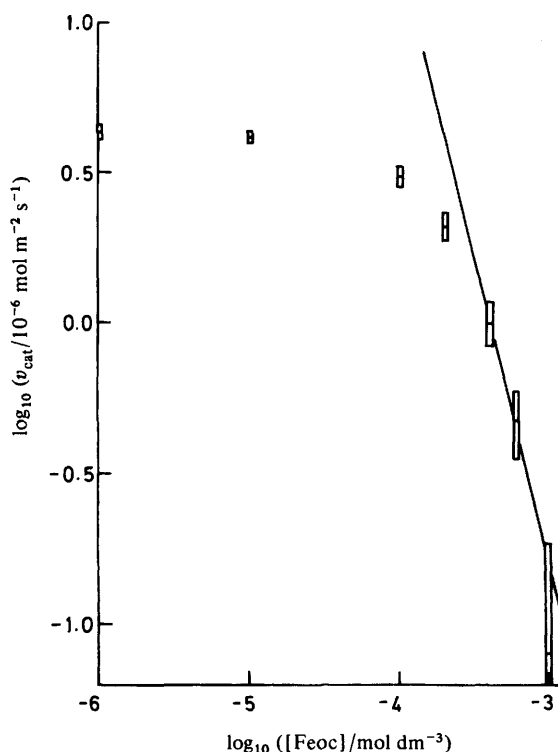


FIG. 3.—Effect of the addition of ferrocyanide on the catalytic rate of the standard reaction mixture at 5 °C. The straight line has been drawn with a slope of -2 .

TABLE 6.—EFFECT ON v_{cat} AND E_{cat} OF THE ADDITION OF IODINE IN $1 \text{ mol dm}^{-3} \text{ KNO}_3$ AT 5 °C AND AT 500 rev. min^{-1}

$[Feic]$ $/10^{-3} \text{ mol dm}^{-3}$	$[I^-]$ $/10^{-3} \text{ mol dm}^{-3}$	$[I_3^-]$ $/10^{-3} \text{ mol dm}^{-3}$	v_{cat} $/10^{-6} \text{ mol m}^{-2} \text{ s}^{-1}$	E_{cat} $/\text{mV}$	E_{cat}^{calc} $/\text{mV}$	E_1^{calc} $/\text{mV}$
1.0	37	0.01	2.89	303	302	281
1.0	37	0.03	2.73	305	305	294
1.0	37	0.05	1.95	306	308	300
1.0	50	0.01	4.27	294	295	270
1.0	50	0.03	3.71	297	297	283
1.0	50	0.05	3.50	298	299	289

except at the lowest Feoc concentrations, E_{cat} is close to the reversible potential E_2 of the Feic/Feoc couple as calculated from the Nernst equation with bulk concentrations. The explanation is that the current-voltage curve of the couple becomes much steeper in the presence of more Feoc, and E_{mix} then lies near E_2 .

Table 6 shows the effect of adding the other product, iodine, to the reaction mixture. The concentration range that could be explored was limited by the high optical absorbances in both sample and reference cells and the consequent instability in the

small differences. Even so, plots of $\log v_{\text{cat}}$ against $\log [I_3^-]$ are consistent with the predicted slope of $-\frac{1}{2}$ (table 4), in contrast to the homogeneous reaction whose rate was unaffected by iodine addition. The experimental E_{cat} values also agree well with those calculated from the theoretical eqn (26a) of ref. (1). Agreement with E_1 , the Nernst potential of the I_3^-/I^- couple, becomes better as the iodine concentration rises and with it the slope of the couple's current-voltage curve.

TABLE 7.—EFFECT OF CHANGING KNO_3 CONCENTRATION AT 5 °C

$[KNO_3]$ /mol dm ⁻³	v_{cat}^a /10 ⁻⁶ mol m ⁻² s ⁻¹	E_1°/V	E_2°/V	$(E_2^\circ - E_1^\circ)$ /V ^b	$10^5 W/FK^{\frac{1}{2}}$ /mol m ⁻² s ⁻¹
0.5	3.29	0.2951	0.2430	-0.0523	1.55
1.0	4.43	0.3000	0.2598	-0.0404	1.55
1.5	4.98	0.2980	0.2638	-0.0343	1.50

^a For 1×10^{-3} mol dm⁻³ Feic + 0.05 mol dm⁻³ KI at 500 rev. min⁻¹; ^b directly measured difference.

A few kinetic and e.m.f. experiments were carried out to investigate the effect of changing the supporting electrolyte concentration. The results are summarised in table 7. To discover to what extent the changes in the formal potentials were responsible for the increases in the catalytic rates, the latter were used to calculate W/F by eqn (10) and then, guided by eqn (11), the products

$$\frac{W}{F} \exp \frac{-2F(E_2^\circ - E_1^\circ)}{3RT}.$$

These are listed in the last column of table 7 and are seen to be quite constant. It follows that the mass-transport rate constants k in eqn (11) do not change significantly when $[KNO_3]$ rises, presumably because the effects of decreasing viscosity and of increasing ionic strength roughly balance each other. It is certainly clear that the variations in the formal potentials, and hence in the equilibrium constant K , override the effects of all the rheological variations. The underlying cause of the rise in both E_2° and v_{cat} probably lies in the increased ion-pairing between K^+ and Feic and Feoc ions.

VARIATION WITH TEMPERATURE

Table 8 shows that the catalytic rate of the standard reaction mixture decreases with rising temperature. The Arrhenius plot is linear and gives an activation energy of -16.9 kJ mol⁻¹. Surprising though this negative activation energy may be, it is in fact predicted by the theory of total mass-transport control. Taking $v_{\text{cat}} \approx W/F$, we see from eqn (11) that the activation energy is composed of a transport term and a thermodynamic term:

$$E_{\text{cat}}^\ddagger = -\frac{R}{3} \frac{\partial \ln(k_{I_3^-} k_{\text{Feoc}}^2)}{\partial(1/T)} - \frac{2F}{3} \frac{\partial[(E_2^\circ - E_1^\circ)/T]}{\partial(1/T)}. \quad (12)$$

It follows from eqn (5) and (10) of ref. (1) and from the Stokes-Einstein equation, eqn (9), that

$$k_{I_3^-} k_{\text{Feoc}}^2 \propto D_{I_3^-}^\ddagger D_{\text{Feoc}}^\ddagger v^{-\frac{1}{2}} \propto (T/\eta)^2 v^{-\frac{1}{2}} \quad (13)$$

TABLE 8.—CATALYTIC RATES AND SOLUTION PROPERTIES AT VARIOUS TEMPERATURES IN 1 mol dm⁻³ KNO₃

<i>T</i> /K	v_{cat}^a /10 ⁻⁶ mol m ⁻² s ⁻¹	η^b /10 ⁻³ kg m ⁻¹ s ⁻¹	ρ^b /kg m ⁻³
273.15	—	1.624	1062.4
278.15	4.43	—	—
283.15	—	1.217	1060.3
288.15	3.32 ^c	—	—
293.15	3.09	—	—
303.15	2.41	0.7925	1053.6

^a For 1 × 10⁻³ mol dm⁻³ Feic + 0.05 mol dm⁻³ KI at 500 rev. min⁻¹; ^b for 1 mol kg⁻¹ KNO₃ (ca. 0.96 mol dm⁻³ KNO₃); ^c $E_{\text{cat}} = 290$ mV (against SCE at 15 °C).

where only the temperature-dependent terms have been included and where the effective radius r of the species has been presumed constant over the temperature range involved. Viscosity data for concentrated KNO₃ solutions at low temperatures are sparse, and we shall therefore employ the figures available for 1 mol kg⁻¹ solutions¹⁹ listed in table 8 together with the appropriate interpolated densities²⁰ to give the kinematic viscosities $\nu (= \eta/\rho)$. Insertion of these figures into eqn (13) allows the transport contribution to the activation energy in eqn (12) to be evaluated: it is +15.2 kJ mol⁻¹. From the slope of a plot of $(E_2^\circ - E_1^\circ)/T$ against $1/T$ using the independently measured potentials in table 2 we find that the thermodynamic contribution to E_{cat} is -32.3 kJ mol⁻¹. Thus

$$E_{\text{cat}}^{\neq \text{calc}} = +15.2 - 32.3 = -17.1 \text{ kJ mol}^{-1}.$$

When the various assumptions made in this calculation are borne in mind, we must conclude that the agreement with the experimental value of -16.9 kJ mol⁻¹ is remarkably good.

COMPARISON OF KINETIC AND ELECTROCHEMICAL EXPERIMENTS

Good concordance between the measured catalytic rates and catalyst potentials on the one hand, and those obtained from independent and purely electrochemical experiments on the other, has already been reported for the present system at 0 °C by Spiro and Griffin.⁸ It remains to confirm this agreement for the exact conditions used here. In both kinetic and electrochemical experiments the platinum disc was preconditioned in the same way: it acted as the catalyst for the former and as the electrode for the latter. Typical current-voltage curves for the Feic/Feoc and I₃⁻/I⁻ couples, drawn with all currents taken as positive, are shown in fig. 4. By the additivity assumption, their point of intersection marks the mixture potential E_{mix} and the mixture current I_{mix} . The circle in fig. 4 marks the potential E_{cat} and the current $I_{\text{cat}} (= FA v_{\text{cat}}$, where A is the catalyst area) determined in the corresponding catalytic runs (table 9). The catalytic point and the electrochemical intersection point, while not exactly coincident, are sufficiently close to lend powerful support to the electrochemical mechanism postulated for the catalysis. Table 9 summarises the result of this and another similar set of experiments. In all of them the agreement between v_{cat} and I_{mix}/FA , and between E_{cat} and E_{mix} , is good.

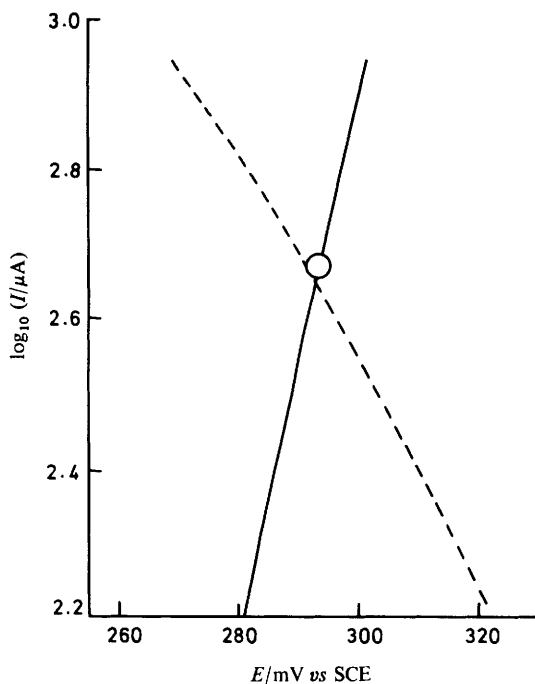


FIG. 4.—Current-potential curves for $1 \times 10^{-3} \text{ mol dm}^{-3} \text{ Feic} + 2 \times 10^{-6} \text{ mol dm}^{-3} \text{ Feoc}$ (----) and for $0.05 \text{ mol dm}^{-3} \text{ KI} + 1 \times 10^{-6} \text{ mol dm}^{-3} \text{ I}_3^-$ (—), both in $1 \text{ mol dm}^{-3} \text{ KNO}_3$ at 5°C with a rotation speed of $500 \text{ rev. min}^{-1}$. The circle marks the average rate and catalyst potential in the corresponding standard catalytic runs between $1 \times 10^{-3} \text{ mol dm}^{-3} \text{ Feic}$ and $0.05 \text{ mol dm}^{-3} \text{ KI}$ in $1 \text{ mol dm}^{-3} \text{ KNO}_3$ at 5°C and $500 \text{ rev. min}^{-1}$.

TABLE 9.—COMPARISON OF RESULTS FROM CATALYTIC AND ELECTROCHEMICAL RUNS WITH $1 \times 10^{-3} \text{ mol dm}^{-3} \text{ Feic}$ AND $0.05 \text{ mol dm}^{-3} \text{ KI}$ IN $1 \text{ mol dm}^{-3} \text{ KNO}_3$ AT 5°C^a

$f/\text{rev. min}^{-1}$	$v_{\text{cat}} / 10^{-6} \text{ mol m}^{-2} \text{ s}^{-1}$	$E_{\text{cat}} / \text{mV}$	$I_{\text{mix}}/FA / 10^{-6} \text{ mol m}^{-2} \text{ s}^{-1}$	$E_{\text{mix}} / \text{mV}$
100	2.00 ± 0.13 (3)	293 ± 1 (3)	2.09 ± 0.02 (2)	293 ± 0.5 (2)
500	4.43 ± 0.05 (5)	295 ± 0.1 (5)	4.21 ± 0.13 (5)	294 ± 0.4 (5)

^a Numbers in brackets refer to the number of runs carried out, and the uncertainty limits are the standard derivations.

CONCLUSIONS

The present paper has described the most thorough study to date of a heterogeneously catalysed redox reaction in solution. That v_{cat} is always proportional to $\sqrt{\omega}$, and E_{cat} independent of it, proved that the catalytic reaction is under total mass-transport control. As complementary evidence it has been found that the potentials adopted by the catalyst are those to be expected if the $\text{Feic} + \text{I}^-$ reaction had rapidly come to equilibrium at the platinum surface. Moreover, the agreement between the directly measured catalytic rates and potentials and those determined by separate electro-

chemical experiments could hardly be explained other than by the electrochemical model of electron transfer through the metal, and indeed many other predictions of this model have been borne out within experimental error. Among these are the values of the initial catalytic rates, the kinetic orders of the reactants, and the marked changes in these orders when one of the products is added at the beginning. Finally, the negative activation energy of the heterogeneous reaction has been explained both in sign and magnitude by the theory based on this model. All the criteria mentioned in the previous paper¹ have therefore been met. We may safely conclude that the mechanism of this reaction – that between ferricyanide and iodide in aqueous KNO₃ solution at an anodised platinum surface – has now been established beyond peradventure.

We thank CONICIT, Venezuela, for the award of a Graduate Fellowship to P.L.F.

- ¹ Part 22.—P. L. Freund and M. Spiro, *J. Chem. Soc., Faraday Trans. 1*, 1983, **79**, 481.
- ² G. Just, *Z. Phys. Chem.*, 1908, **63**, 513.
- ³ G. M. Waind, *Chem. Ind. (London)*, 1955, 1388.
- ⁴ M. Spiro, *J. Chem. Soc.*, 1960, 3678.
- ⁵ M. Spiro, R. R. M. Johnston and E. S. Wagner, *Electrochim. Acta*, 1961, **3**, 264.
- ⁶ M. Spiro and A. B. Ravnö, *J. Chem. Soc.*, 1965, 78, and unpublished work.
- ⁷ Y. A. Majid and K. E. Howlett, *J. Chem. Soc. A*, 1968, 679, and personal communication.
- ⁸ M. Spiro and P. W. Griffin, *Chem. Commun.*, 1969, 262, and unpublished work.
- ⁹ J. M. Austin, T. Groenewald and M. Spiro, *J. Chem. Soc., Dalton Trans.*, 1980, 854.
- ¹⁰ V. G. Levich, *Physicochemical Hydrodynamics* (Prentice-Hall, Englewood Cliffs, N.J., 1962), p. 69.
- ¹¹ A. C. Riddiford, *Adv. Electrochem. Electrochem. Eng.*, 1966, **4**, 47.
- ¹² D. Gilroy, *J. Electroanal. Chem.*, 1976, **71**, 257.
- ¹³ L. I. Katzin and E. Gebert, *J. Am. Chem. Soc.*, 1955, **77**, 5814.
- ¹⁴ W. L. Reynolds, *J. Am. Chem. Soc.*, 1958, **80**, 1830.
- ¹⁵ C. Wagner, *Z. Phys. Chem.*, 1924, **113**, 261.
- ¹⁶ *Stability Constants of Metal-ion Complexes*, ed. L. G. Sillén and A. E. Martell (Special Publication, The Chemical Society, London, 1964), vol. 17; 1971, vol. 25.
- ¹⁷ R. A. Robinson and R. H. Stokes, *Electrolyte Solutions* (Butterworths, London, 2nd edn, 1959), Appendix 8.10.
- ¹⁸ S. Z. Hussain, *Ph.D. Thesis* (University of London, 1979); K. E. Howlett, personal communication.
- ¹⁹ G. Tamman and H. Rabe, *Z. Anorg. Chem.*, 1928, **168**, 73.
- ²⁰ *International Critical Tables*, ed. E. W. Washburn (McGraw-Hill, New York, 1928), vol. III.
- ²¹ M. V. Stackelberg, M. Pilgram and V. Toome, *Z. Elektrochem.*, 1953, **57**, 342.
- ²² D. Jahn and W. Vielstich, *J. Electrochem. Soc.*, 1962, **109**, 849.
- ²³ A. J. Arvia, J. C. Bazán and J. S. W. Carrozza, *Electrochim. Acta*, 1968, **13**, 81.
- ²⁴ A. J. Arvia, S. L. Marchiano and J. J. Podestá, *Electrochim. Acta*, 1967, **12**, 259.
- ²⁵ S. L. Gordon, J. S. Newman and C. W. Tobias, *Ber. Bunsenges. Phys. Chem.*, 1966, **70**, 414.
- ²⁶ R. Mills and J. W. Kennedy, *J. Am. Chem. Soc.*, 1953, **75**, 5696.
- ²⁷ H. G. Hertz, M. Holz and R. Mills, *J. Chim. Phys.*, 1974, **71**, 1355.
- ²⁸ R. H. Stokes, L. A. Woolf and R. Mills, *J. Phys. Chem.*, 1957, **61**, 1634.
- ²⁹ R. H. Stokes and R. Mills, *Viscosity of Electrolytes and Related Properties* (Pergamon, Oxford, 1965), Appendices.